Stable Organic Radicals

DOI: 10.1002/anie.201410796

Isolation of a Hydrogen-Bonded Complex Based on the Anthranol/Anthroxyl Pair: Formation of a Hydrogen-Atom Self-Exchange System**

Yasukazu Hirao, Tohru Saito, Hiroyuki Kurata, and Takashi Kubo**

Abstract: *A hydrogen-bonded complex was successfully isolated as crystals from the anthranol/anthroxyl pair in the self-exchange proton-coupled electron transfer (PCET) reaction. The anthroxyl radical was stabilized by the introduction of a 9-anthryl group at the carbon atom at the 10-position. The hydrogen-bonded complex with anthranol self-assembled by π–π stacking to form a one-dimensional chain in the crystal. The conformation around the hydrogen bond was similar to that of the theoretically predicted PCET activated complex of the phenol/phenoxyl pair. X-ray crystal analyses revealed the self-exchange of a hydrogen atom via the hydrogen bond, indicating the activation of the self-exchange PCET reaction between anthranol and anthroxyl. Magnetic measurements revealed that magnetic ordering inside the one-dimensional chain caused the inactivation of the self-exchange reaction.*

Electron-transfer reactions involving proton-transfer processes are usually discussed in terms of the proton-coupled electron transfer (PCET) mechanism.[1] Such reactions are widely found in chemical and biological systems. For example, the electron transfer in photosystem II (PSII)[2] and ribonucleotide reductase (RNR)[3] were reported to be driven by the PCET mechanism. In both cases, the oxidation of phenol is a key step.[4] Phenol releases a proton and an electron and is converted into phenoxyl. The coupling of proton-transfer processes to electron-transfer processes reduces the activation barrier of these reactions. The nature of PCET reactions has attracted interest of researchers in the field of organic conductors in the course of exploring superconducting molecular materials. A quinhydrone complex, consisting of *para*-hydroquinone and *para*-benzoquinone, was one of the first examples of PCET activated molecular conductors. It exhibited electron transfer via π–π stacking coupled with proton transfer through the hydrogen bonds under high-pressure conditions.[5] Recently, Mori et al. reported a similar type of the complex based on catechol-fused[6a–c] or pyridyl-substituted[6d] tetrathiafulvalene (TTF) derivatives. They observed the proton–electron coupled state.

Herein, we investigated the self-exchange system of PCET reactions between phenol and phenoxyl. Theoretical studies on this self-exchange reaction have been reported.[7,8] These studies revealed the possibility of the presence of a concerted reaction of the proton and electron transfer based on quantum calculations and reaction energy discussions. At the theoretically predicted transition state, phenol and phenoxyl form a head-to-head hydrogen bond. The orbital analyses of this self-exchange system revealed the transfer pathway of the proton and electron. Proton transfer is expected to occur through the overlap of the lone pair of electrons on the oxygen atoms, whereas an electron transfers through the overlap of π-orbitals distributed on oxygen atoms. Both overlaps are found in the hydrogen bond. Based on these studies, we envision that the hydrogen bond in the phenol/phenoxyl pair can be regarded as a conductive path rather than a dielectric path. We synthesized and isolated a PCET activated complex in the crystalline form to verify the conductive hydrogen bonds experimentally.

One of the largest barriers to observing the hydrogen-bonded complex between phenol and phenoxyl is the stability of phenoxyl. Usually, phenoxyl is stabilized by the introduction of sterically bulky groups (that is, *tert*-butyl) at the 2,4,6-positions having a high spin density. However, the bulky *tert*-butyl groups at the 2- and 6-positions can inhibit the formation of the hydrogen bond. To address this, a new stable phenoxyl derivative was designed. Anthroxyl is thought to be a suitable radical for this purpose. Instead of bulky groups, the extension of the π-conjugated system of the anthracene ring of anthroxyl is expected to increase the stability of the radical. Furthermore, the empty space around the oxygen atom favors the formation of a rigid hydrogen bond. We decided to introduce a bulky anthryl group at the 10-position of anthroxyl (Scheme 1) to increase the stability, because of the relatively high spin density at that position. The anthryl-substituted anthroxyl radical (**1**), which was generated by the oxidation of bianthryl, has only been characterized by electron spin resonance (ESR) spectroscopy.[9] We synthesized this anthroxyl derivative **1** by a multi-

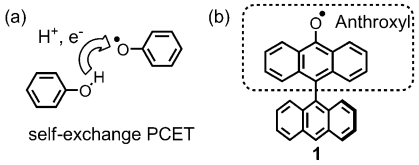

Scheme 1. a) The self-exchange PCET reaction between phenol and phenoxyl pair. b) Anthryl-substituted anthroxyl **1**.

[*] Dr. Y. Hirao, T. Saito, Prof. Dr. H. Kurata, Prof. Dr. T. Kubo
Department of Chemistry, Graduate School of Science
Osaka University, Toyonaka, Osaka 560-0043 (Japan)
E-mail: y-hirao@chem.sci.osaka-u.ac.jp

[**] This work was supported in part by Scientific Research on Innovative Areas by MEXT, "Stimuli-responsive Chemical Species for the Creation of Functional Molecules" (No.2408).

Supporting information for this article is available on the WWW under http://dx.doi.org/10.1002/anie.201410796.

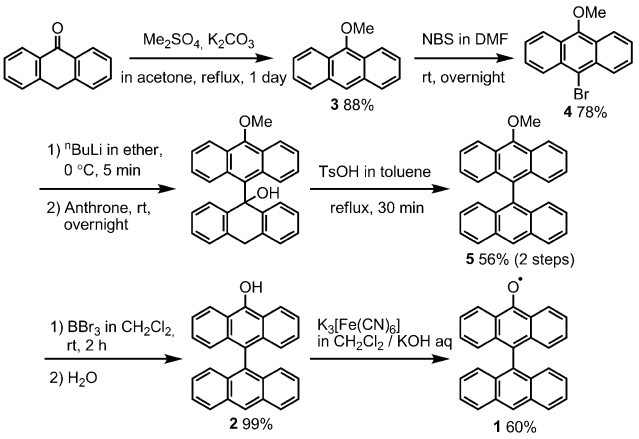

Scheme 2. Synthetic route to anthryl-substituted anthroxyl **1**.

step reaction, and its reduced form anthranol (**2**) for the construction of a PCET activated complex, and then isolated the complex in the crystalline form.

The synthetic route to **1** is shown in Scheme 2. Starting from anthrone, methylation followed by bromination provided 9-bromo-10-methoxylanthracene (**4**) in good yield. Thereafter, the coupling reaction with anthrone and subsequent dehydroxylation afforded methoxybianthryl (**5**). After demethylation with BBr_3, the resulting anthranol **2** was oxidized with potassium ferricyanide to form 9-anthryl-substituted anthroxyl **1**. The stability of **1** was found to be very high; **1** was stable even when it was treated with a polar protic solvent, such as alcohol or water, in air. Because of the high stability of **1**, pure **1** was obtained as brown platelet crystals from a toluene solution. X-ray crystallographic analysis indicated that the carbon atom at the 10-position, with high spin density, was sandwiched from top and bottom by the two hydrogen atoms at the *peri* positions of the orthogonally substituted anthracene ring (Supporting Information, Figure S1). This structural feature is important for stabilizing the radical. The phenyl-substituted derivative could not be isolated. The absence of steric repulsion allows the phenyl ring to rotate and the protection of the spin center is insufficient. The hyperfine splitting of the solution ESR spectrum of **1** was mainly derived from the hydrogen atoms at the 2,4,5,7-positions of anthroxyl (Supporting Information, Figure S2). We did not find significant leaks of the spin density into the anthracene substituent. The delocalized spin distribution of the anthroxyl radical was in agreement with that estimated from quantum calculations. The redox property of **1** was evaluated by cyclic voltammetry in dichloromethane solution. The voltammogram showed two reversible waves at −0.86 V and 0.40 V (vs. Fc/Fc^+; Supporting Information, Figure S3). The lower redox wave can be assigned to the electron-reduction process from the radical to the anion, and the higher wave corresponds to the oxidation process from the radical to the cation. The detailed description of the ESR analyses and the temperature dependent superconducting quantum interference device (SQUID) measurements is given in the Supporting Information.

A hydrogen-bonded complex between anthroxyl **1** and its reduced form, anthranol **2**, was successfully isolated. The

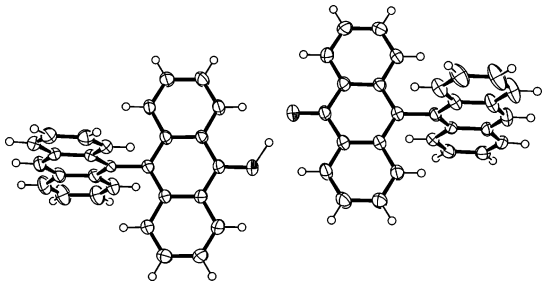

Figure 1. X-ray structure of the hydrogen-bonded complex between **1** and **2** at 100 K.[12] Ellipsoids are set at 50% probability.

mixing of **1** and **2** in toluene and subsequent slow evaporation gave brown platelet crystals suitable for X-ray crystallographic analysis.[12] The shape and color of the crystals were similar to those of **1**. Single-crystal X-ray analysis at 100 K showed that **1** and **2** were almost coplanar and faced each other in the form of O···HO (Figure 1; Supporting Information, Table S1). Such a hydrogen-bonded complex in the solid state has thus far been rarely observed.[6a,c] One of the C–O bond lengths was 1.340(2) Å, which is a typical value for phenols, suggesting that the hydrogen atom in the hydrogen bond was completely localized on the alcohol. The intermolecular O···O distance was determined to be 2.767(3) Å, which is close to the theoretically predicted value (2.799 Å) for the hydrogen-bonded complex of the phenol/phenoxyl pair.[10]

To observe the self-exchange reaction, the X-ray structural analysis was also performed at higher temperature (Supporting Information, Table S2).[12] As summarized in Table S5, the cell parameters at 200 K are quite different from those at 100 K. For instance, the cell volume decreased to half its original value. The X-ray structural analysis at 200 K was carried out by using this new unit cell. The radical and the alcohol became indistinguishable from each other in the resulting structure. The C–O bond length was observed to be 1.305 Å, which is close to the average bond length of **1** and **2** (Table S3). This averaging phenomenon results in an inversion center between **1** and **2**, which subsequently leads to the volume reduction of the unit cell to half the original volume.

A difference Fourier map generated using the ShelXle program[11] can be used to visualize the electron distribution map of the hydrogen atom involved in the hydrogen bond and provide useful information about the behavior of the hydrogen atom. At 100 K, the hydrogen atom was localized on alcohol **2**. However, as shown in Figure 2, the observed electron density from the hydrogen atom splits into two centers at 200 K. This distribution map suggested hydrogen atom-hopping on a double-minimum potential. According to these analyses, a thermally activated self-exchange reaction, involving a hydrogen atom exchange between anthranol and anthroxyl, resulted in the averaged structure observed at 200 K. Compared with the theoretically predicted model of the phenol/phenoxyl pair, the similar conformation around the hydrogen bond suggests that the self-exchange reaction occurring in the anthranol/anthroxyl pair is a concerted PCET reaction.[7] The intermolecular O···O distance at 200 K was determined to be 2.758(3) Å, which was longer than the value (2.4 Å) predicted for the transition state of the phenol/

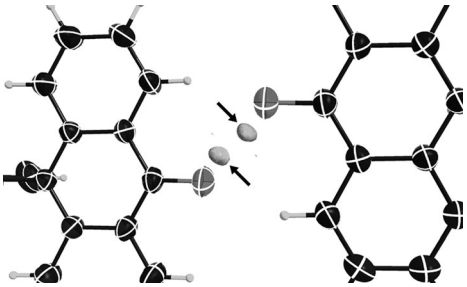

Figure 2. Difference Fourier map (indicated by arrows) of electron density around the hydrogen bond in the hydrogen-bonded complex between **1** and **2** at 200 K. The electron density of split hydrogen atoms in the O···O bond was observed.

phenoxyl pair.[7] This may be attributed to steric interactions between O and the C–H of the neighboring molecule.

The transition observed by X-ray analysis was also investigated in detail from the perspective of the magnetic structure. SQUID measurements on the crystalline powder were expected to be a powerful tool for understanding the phase transition. The temperature dependence of the molar magnetic susceptibility (χ_m) was measured in the temperature range 2–300 K at a constant field of 1 T (Figure 3). The $\chi_m T$

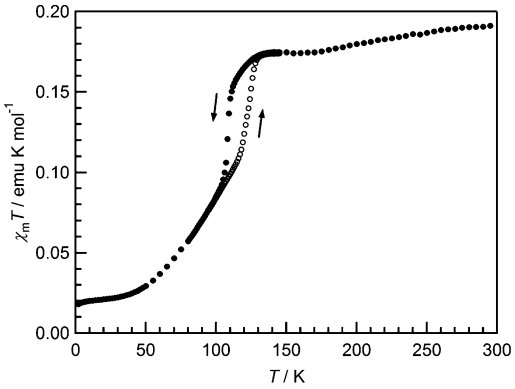

Figure 3. Temperature dependence of $\chi_m T$ of the crystalline powder sample of the hydrogen-bonded complex between **1** and **2** under a constant magnetic field of 1 T.

value of 0.19 emu K mol^{-1} at 300 K was close to the theoretical value of 0.375/2 emu K mol^{-1} for the isolated $S = 1/2$ spin of anthroxyl, which accounts for half of the molecules. Remarkably, the $\chi_m T$ versus T plot showed a striking and irregular decrease of $\chi_m T$ at approximately 125 K. This transition exhibited a thermal hysteresis of about 15 K between cooling and heating runs, which is an indication of a first-order magnetic phase transition. We suspect this transition is related to the structural change observed in the X-ray analysis. The two X-ray structures obtained at 100 K and 200 K are considered to be the structures below and above this phase transition temperature, respectively. From this measurement, the inactivity of the self-exchange reaction at 100 K is ascribed not simply to the height of the self-exchange reaction barrier, but also to a phase transition.

The behavior of the molar magnetic susceptibility can be understood through the intermolecular interactions observed in the crystal. The crystal packing structure of the hydrogen-bonded complex contains a one-dimensional chain structure composed of two intermolecular interactions. One is an O•···HO hydrogen bonding interaction between anthranol and the anthroxyl; the other is a π–π stacking interaction between the planar anthroxyl/anthranol regions. The hydrogen-bonded dimer was stacked together via the π–π interaction to form an offset one-dimensional chain as depicted in Figure 4. At 100 K, the sequence of radical **1** and alcohol **2** in

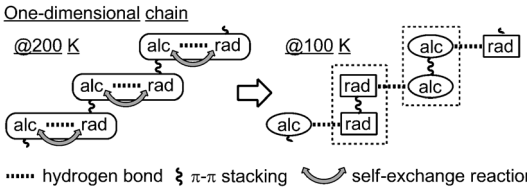

Figure 4. Representation of the hydrogen-atom exchange within the one-dimensional chain of the hydrogen-bonded complex. Anthranol and anthroxyl are abbreviated as "alc" and "rad", respectively. Alc and rad are indistinguishable in the hydrogen-bonded complex at 200 K and their positions are unclear.

the chain was uniquely determined by X-ray analysis (Figure 5a). Compounds **1** and **2** were distinguished on the basis of the C–O bond length. The π–π separation distance d of the overlapping anthroxyls was 3.395 Å, whereas anthranol formed a weak π–π stacking pair ($d = 3.544$ Å). We could not determine the sequence at 200 K (Figure 5b). Only the averaged structure of **1** and **2** was obtained by the X-ray analysis as mentioned earlier, and the hydrogen-bonded complex formed a uniform stack with $d = 3.497$ Å along the chain. The presence of a hydrogen bond was confirmed by a broad signal around 3300 cm^{-1} (ν_{O-H}) in the infrared (IR)

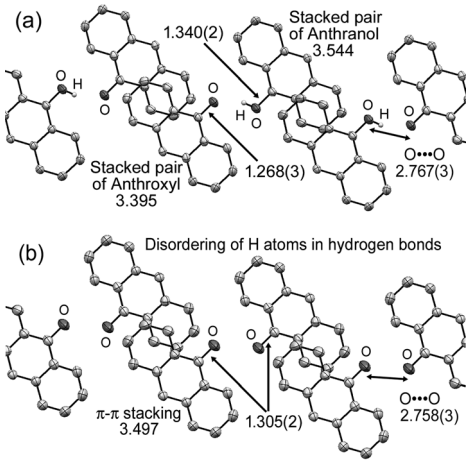

Figure 5. Crystal packing structure of the hydrogen-bonded complex between **1** and **2** at a) 100 K and b) 200 K. Ellipsoids are set at 50% probability; substituted-anthracene and the carbon-bound hydrogen atoms are omitted for clarity. The C–O bond length and π–π separation distances are shown in Å. The hydrogen atom within the O–H···O at 200 K is omitted owing to disordering.

spectrum measured at 300 K (Supporting Information, Figure S6).

Concurrent with these changes in the molecular arrangement, the magnetic phase transition observed at 125 K can be associated with phase transition from the disordered to the ordered state. The formation of the strongly stacked radical pair ceases the self-exchange reaction, and results in the localization of the hydrogen atom. The decrease of $\chi_m T$ at the phase transition can be ascribed to the antiferromagnetic interaction of the stacked radical pairs, which is thought to be the driving force for the phase transition (Figure 4). The other two behaviors of the $\chi_m T$ versus T plot, namely the gradual decrease of $\chi_m T$ at the high temperature region and the non-zero value of $\chi_m T$ at a very low temperature, were thought to stem from a mismatch of the sequence in the chain or from the radical located on the terminus of the chain. Because the crystal packing of the hydrogen-bonded complex is very similar to that of the radical alone (Supporting Information, Figure S5), an alcohol molecule may be substituted by a radical. In this mismatched region, there is no hydrogen atom exchange, and an antiferromagnetic interaction from the aggregated radicals can occur.

We conclude that the hydrogen-atom self-exchange reactions, based on the PCET mechanism between anthranol and anthroxyl, are inactive during the phase transition because of the strong antiferromagnetic pairing of the radicals inside the one-dimensional chain. The temperature-induced phase transition is reversible and is activated again at high temperature. However, the C=O IR stretching vibration of anthroxyl and the O–H vibration of anthranol at 300 K and 5 K (Supporting Information, Figure S6) provide no direct evidence for the exchange (such as an anomalous peak shift). The timescale for the exchange reaction is probably slow. Further investigations about the dynamics are currently in progress.

The high stability of anthroxyl radical **1** allowed us to isolate a hydrogen-bonded complex with anthranol **2**, which was found to be active in the self-exchange reaction. The electron distribution map of the hydrogen atom confirmed the activation of this reaction. Also, the X-ray structure of our hydrogen-bonded complex was close to that of the predicted PCET activated complex of the phenol/phenoxyl pair. Kinetic studies in the solution phase and theoretical studies examining PCET reactions[7,8] will be supplemented with the structural information in this solid-phase study. We envision shorter hydrogen bond lengths are necessary for activating the PCET reaction, and we will prepare modified anthroxyls aimed at generating more efficient PCET systems. Furthermore, we will conduct experimental studies to compare with the theoretical prediction and relate these findings to the application of PCET reactions as a new conductive mechanism for organic conductors.

Received: November 5, 2014
Published online: January 7, 2015

Keywords: aryloxyl radical · hydrogen bonds · organic conductors · proton-coupled electron transfer · stable organic radicals

[1] a) J. J. Warren, T. A. Tronic, J. M. Mayer, *Chem. Rev.* **2010**, *110*, 6961 – 7001; b) S. Hammes-Schiffer, A. A. Stuchebrukhov, *Chem. Rev.* **2010**, *110*, 6939 – 6960; c) M. H. V. Huynh, T. J. Meyer, *Chem. Rev.* **2007**, *107*, 5004 – 5064; d) C. Costentin, M. Robert, J.-M. Savéant, *Chem. Rev.* **2010**, *110*, PR1 – PR40.

[2] a) H. J. Eckert, G. Renger, *FEBS Lett.* **1988**, *236*, 425 – 431; b) C. W. Hoganson, G. T. Babcock, *Science* **1997**, *277*, 1953 – 1956; c) H. Matsuoka, J.-R. Shen, A. Kawamori, K. Nishiyama, Y. Ohba, S. Yamaguchi, *J. Am. Chem. Soc.* **2011**, *133*, 4655 – 4660.

[3] a) C. S. Yee, M. C. Y. Chang, J. Ge, D. G. Nocera, J. Stubbe, *J. Am. Chem. Soc.* **2003**, *125*, 10506 – 10507; b) J. Stubbe, D. G. Nocera, C. S. Yee, M. C. Y. Chang, *Chem. Rev.* **2003**, *103*, 2167 – 2201.

[4] C. Costentin, C. Louault, M. Robert, J.-M. Savéant, *J. Am. Chem. Soc.* **2008**, *130*, 15817 – 15819.

[5] a) T. Mitani, G. Saito, H. Urayama, *Phys. Rev. Lett.* **1988**, *60*, 2299 – 2302; b) K. Nakasuji, K. Sugiura, T. Kitagawa, J. Toyoda, H. Okamoto, K. Okaniwa, T. Mitani, H. Yamamoto, I. Murata, A. Kawamoto, J. Tanaka, *J. Am. Chem. Soc.* **1991**, *113*, 1862 – 1864.

[6] a) T. Isono, H. Kamo, A. Ueda, K. Takahashi, A. Nakao, R. Kumai, H. Nakao, K. Kobayashi, Y. Murakami, H. Mori, *Nat. Commun.* **2013**, *4*, 1344; b) H. Kamo, A. Ueda, T. Isono, K. Takahashi, H. Mori, *Tetrahedron Lett.* **2012**, *53*, 4385 – 4388; c) A. Ueda, S. Yamada, T. Isono, H. Kamo, A. Nakao, R. Kumai, H. Nakao, Y. Murakami, K. Yamamoto, Y. Nishio, et al., *J. Am. Chem. Soc.* **2014**, *136*, 12184 – 12192; d) S. C. Lee, A. Ueda, H. Kamo, K. Takahashi, M. Uruichi, K. Yamamoto, K. Yakushi, A. Nakao, R. Kumai, K. Kobayashi, H. Nakao, Y. Murakami, H. Mori, *Chem. Commun.* **2012**, *48*, 8673 – 8675.

[7] J. M. Mayer, D. A. Hrovat, J. L. Thomas, W. T. Borden, *J. Am. Chem. Soc.* **2002**, *124*, 11142 – 11147.

[8] For other theoretical studies, see; a) A. Sirjoosingh, S. Hammes-Schiffer, *J. Phys. Chem. A* **2011**, *115*, 2367 – 2377; b) M. K. Ludlow, J. H. Skone, S. Hammes-Schiffer, *J. Phys. Chem. B* **2008**, *112*, 336 – 343; c) J. H. Skone, A. V. Soudackov, S. Hammes-Schiffer, *J. Am. Chem. Soc.* **2006**, *128*, 16655 – 16663; d) G. A. DiLabio, E. R. Johnson, *J. Am. Chem. Soc.* **2007**, *129*, 6199 – 6203.

[9] a) T. Yoshida, Y. Ueno, S. Wakabayashi, *Kogyo Kagaku Zasshi* **1969**, *72*, 338 – 341; b) L. S. Singer, I. C. Lewis, T. Richerzhagen, G. Vincow, *J. Phys. Chem.* **1971**, *75*, 290 – 291; c) I. C. Lewis, L. S. Singer, *J. Phys. Chem.* **1981**, *85*, 354 – 360; d) P. Devolder, *Can. J. Chem.* **1976**, *54*, 1744 – 1750; e) P. Devolder, P. Goundmand, *Chem. Phys.* **1978**, *35*, 307 – 315.

[10] See the Supporting Information of Ref. [7].

[11] "ShelXle: a Qt graphical user interface for SHELXL": C. B. Hübschle, G. M. Sheldrick, B. Dittrich, *J. Appl. Crystallogr.* **2011**, *44*, 1281 – 1284.

[12] CCDC 1040627 (100 K) and CCDC 1040628 (200 K) contain the supplementary crystallographic data for this paper. These data can be obtained free of charge from The Cambridge Crystallographic Data Centre via www.ccdc.cam.ac.uk/data_request/cif.

